

$\tau_1$ ,  $\tau_2$ , and  $A$  parameters ( $r \geq 0.96$ ) are set out in Table I. The impressive SHG temporal stability of the I + III cross-linked matrices prompted additional quantitative temporal stability measurements at elevated temperatures. As can be seen in Figure 2 and Table I, the  $d_{33}$  decay (especially the initial decay) is, as expected, more rapid at 85 °C. Nevertheless, the long-term decay time constant is still on the order of 4 months.

These results demonstrate that difunctional chromophoric azo co-monomers which can function as amino components of cross-linkable NLO-active epoxy matrices are synthetically accessible. After concurrent electric field poling and thermal cross-linking with a diepoxide or preferentially, with a polyepoxide, such matrices exhibit high SHG efficiency and SHG efficiency temporal stability.

**Acknowledgment.** We thank the NSF (Grant DMR 8821571) through Northwestern University Materials Research Center and AFOSR (Contract 90-0071) for support of this research. We acknowledge Prof. J. M. Torkelson and Ms. M. A. Firestone for helpful discussions. M.A.H. thanks the AFOSR for a Laboratory Graduate Fellowship.

**Registry No.** I, 142743-67-7; (I)(II) (copolymer), 142743-68-8; (I)(III) (copolymer), 142761-41-9.

(18) Fredrickson, G. H. *Annu. Rev. Phys. Chem.* 1988, 39, 149-180.

## Room-Temperature Synthesis of Molybdenum and Tungsten Carbides, $\text{Mo}_2\text{C}$ and $\text{W}_2\text{C}$ , via Chemical Reduction Methods

D. Zeng and M. J. Hampden-Smith\*

*Department of Chemistry and Center for  
Micro-Engineered Ceramics  
University of New Mexico  
Albuquerque, New Mexico 87131*

*Received April 21, 1992  
Revised Manuscript Received June 8, 1992*

The preparation of nanometer-sized particles of phase-pure materials is currently attracting intense interest in materials chemistry because such particles exhibit unique chemical and physical properties that are intermediate between those of molecules and extended solids.<sup>1</sup> For example, metal chalcogenides exhibit size-dependent physical properties in the 2-100-nm size regime<sup>2</sup> and metal particles exhibit size-dependent selectivity<sup>3</sup> and reactivity<sup>3,4</sup> in catalytic reactions. However, traditional solid-state synthetic methods seldom result in formation of particles smaller than 100 nm.<sup>5</sup> New synthetic routes based on chemical methods show promise for the formation of materials with a homogeneity, morphology, composition, microstructure, and purity not otherwise obtainable. For example, the reduction of metal salts in the presence of a surfactant, often in inverse micelles, has led to formation

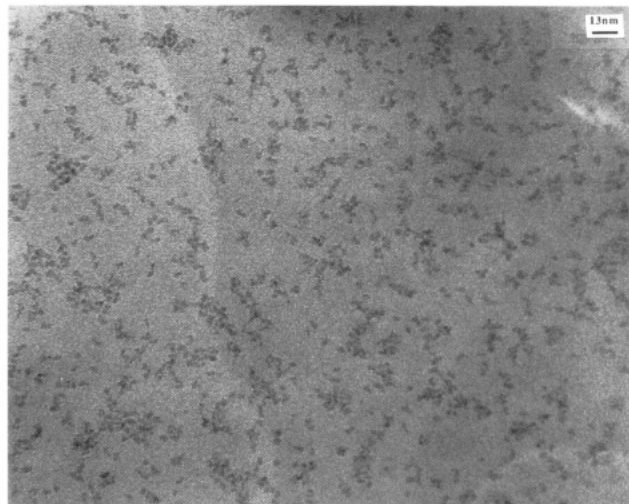


**Figure 1.** TEM data for  $\text{Mo}_2\text{C}$  particles formed by reduction of  $\text{MoCl}_3(\text{THF})_3$  with  $\text{LiBEt}_3\text{H}$  in THF.

of monodispersed nanometer-sized particles.<sup>6</sup> However, the surfactant can lead to impurity incorporation in subsequent steps and as a result a number of groups are investigating alternative synthetic strategies. Reicke et al.<sup>7</sup> have extensively investigated the reduction of metal salts with alkali-metal naphthalenides and formed highly dispersed, reactive metal powders. Bonnemenn et al.<sup>8,9</sup> have shown that trialkylborohydride reducing agents can be used to reduce a variety of metal complexes to form the corresponding metal colloids. The metals are reasonably pure (70-98%), the particle size was approximately 10-100 nm and generally crystalline materials were formed depending on the specific system as determined by X-ray diffraction.

Here we report the room-temperature reduction of molybdenum and tungsten halides with  $\text{LiBEt}_3\text{H}$ , which results in the formation of monodispersed, 1- and 2-nm  $\text{Mo}_2\text{C}$  and  $\text{W}_2\text{C}$  colloids, respectively, rather than formation of the metal. Existing routes to these interstitial carbide materials involve either high temperature (>1200 °C) reduction of the corresponding metal oxide<sup>10-13</sup> or halide<sup>14</sup> or ball-mixing mixtures of elemental powders for extended periods at lower temperatures.<sup>15,16</sup> Both these methods often result in addition reactions between the reagent and container causing impurity incorporation.

The reduction of THF suspensions of  $\text{MoCl}_4(\text{thf})_2$ ,  $\text{MoCl}_3(\text{thf})_3$  and  $\text{WCl}_4$  at -10 °C with a slight excess of the stoichiometric amount of  $\text{LiBEt}_3\text{H}$  resulted in the forma-

(6) Wilcoxon, T. P.; Baughmann, R. J.; Williamson, R. L. *Synthesis and Properties of New Catalysts: Utilization of Novel Materials Components and Synthetic Techniques*. Corcoran, E. W., Ledoux, M. J., Eds.; Fall Materials Research Society Meeting, Boston, MA, 1990 and references therein.

(7) Riecke, R. D. *Science* 1989, 246, 1260. Riecke, R. D.; Burns, T. P.; Wehmeyer, R. M.; Kahn, B. E. In *High Energy Processes in Organometallic Chemistry*; ACS Symposium Series 333; American Chemical Society: Washington, DC, 1987.

(8) Bonnemenn, H.; Brijoux, W.; Jousson, T. *Angew. Chem., Int. Ed. Engl.* 1990, 29, 273.

(9) Bonnemenn, H.; Brijoux, W.; Brinkmann, R.; Dinjus, E.; Jousson, T.; Korall, B. *Angew. Chem., Int. Ed. Engl.* 1991, 30, 1312.

(10) Lee, J. S.; Oyama, S. T.; Boudart, M. *J. Catal.* 1987, 106, 125.

(11) Oyama, S. T.; Schlatter, J. C.; Metcalfe III, J. E.; Lambert, J. M. *Ind. Chem. Res.* 1988, 27, 1639.

(12) Boudart, M.; Oyama, S. T.; Volpe, L. US Patent 4,515,763.

(13) Ranhorta, G. S.; Haddix, G. W.; Bell, A. T.; Reimer, J. A. *J. Catal.* 1987, 108, 24.

(14) Tamari, N.; Kato, A. *Yogyo Kyokaiishi* 1976, 409, 84; *Chem. Abstr.* 85:162594d.

(15) Le Caer, G.; Bauer-Grosse, E.; Pianelli, A.; Bouzy, E.; Matteazzi, P. *J. Mater. Sci.* 1990, 23, 4726.

(16) Matteazzi, P.; Le Caer, G. *J. Am. Ceram. Soc.* 1991, 74, 1382.

\* To whom correspondence should be addressed.

(1) See, e.g. *Frontiers in Materials Science. Science* 1992, 255, 1049 and references therein.

(2) Pool, R. *Science* 1990, 248, 1186 and references therein.

(3) Che, M.; Bennett, C. O. *The Influence of Particle Size on the Catalytic Properties of Supported Metals. Adv. Catal.* 1989, 36, 55. See also: Glassl, H.; Hayek, R.; Kramer, R. *J. Catal.* 1981, 68, 397.

(4) Davis, S. C.; Klabunde, K. J. *Chem. Rev.* 1982, 83, 153.

(5) Chorley, R. W.; Lednor, P. W. *Adv. Mater.* 1991, 3, 474.

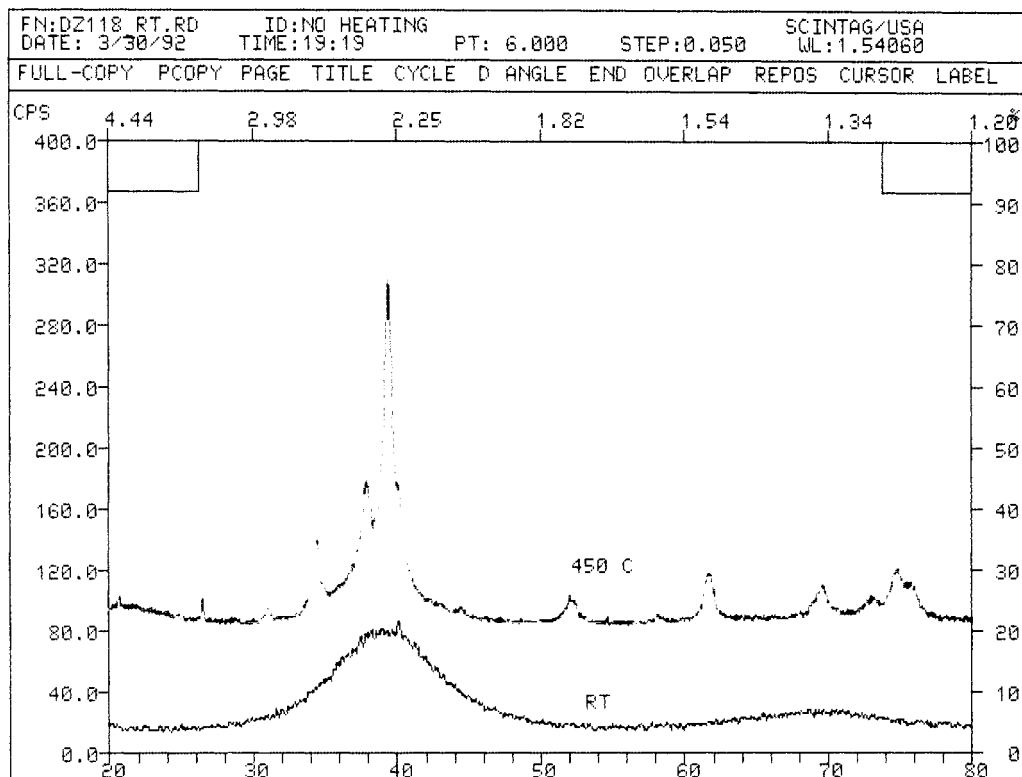


**Figure 2.** Variable-temperature X-ray powder diffraction data for  $W_2C$  showing the growth of the crystallites with increasing temperature and confirming the presence of crystalline  $W_2C$ . The lower X-ray powder pattern was obtained at room temperature. The upper X-ray powder pattern was obtained after heating to 450 °C.

tion of a black solution accompanied by gas evolution.<sup>17</sup> After stirring for 24 h, the colloidal suspensions generally aggregated and black powders could be isolated by centrifugation. Under some conditions, the black powders could be isolated and redispersed in THF to give black colloidal solutions. For  $MoCl_3(THF)_3$ , a representative example, the black powder isolated had a particle size of approximately 1–2  $\mu m$  (SEM) and contained only Mo by energy-dispersive spectroscopy. Closer examination by transmission electron microscopy revealed that the 1–2- $\mu m$  sized particles were agglomerates of smaller, 2-nm-sized particles. Energy-dispersive spectroscopy revealed only Mo and electron diffraction revealed a diffuse ring at a  $d$  spacing corresponding to  $\sim 2.4$  Å, consistent with the very broad peak observed for the same sample by X-ray powder diffraction. TEM of a sample of the same material redispersed in THF revealed the presence of monodispersed particles approximately 2 nm in diameter, Figure 1. This particle size is consistent with the broadening observed by X-ray diffraction as calculated from the Scherrer equation and may represent the crystallite size. However, due to the broadness of the X-ray diffraction peak, it is not clear if the material is amorphous or crystalline at this stage. In addition, because of the similarity between the crystal structures, and therefore the powder diffraction patterns

of Mo and  $Mo_2C$ , a distinction between these species could not be made at this stage. To distinguish these two possibilities, the sample was sintered at a number of different temperatures, in vacuo, to increase the size of the crystallites. On heating to 500 °C, the X-ray diffraction pattern sharpened and corresponded to that of  $Mo_2C$ . No evidence for Mo metal was observed. The X-ray diffraction data for  $W_2C$  as-prepared at room temperature and after heating to 450 °C in vacuo are presented in Figure 2. Higher temperature sintering of  $Mo_2C$  at  $10^{-2}$  Torr resulted in partial oxidation to form traces of crystalline Mo and  $MoO_2$ , as determined in X-ray diffraction, and presumably  $CO_2$ . Thermogravimetric analysis in air quantitatively confirmed this oxidation to  $MoO_2$  via an observed weight gain of 25% (calculated, 26%). The oxidation of Mo would have resulted in a weight gain of 36% for the analogous oxidation reaction.

Similar observations were made for the formation of  $Mo_2C$  from  $MoCl_4(thf)_2$  and  $W_2C$  from  $WCl_4$ . The interstitial carbides were formed in high yields (>93%) and were all composed of 1–2-nm-sized primary crystallites which sintered to enable unambiguous phase assignment at 450–500 °C. The presence of carbon in all as-prepared samples prior to sintering was confirmed by combustion elemental analysis. The origin of the carbide has not been identified at this stage. However, evidence that it is incorporated in the initial reaction rather than in a subsequent washing and isolation step comes from a separate experiment in which the crude, centrifuged, aggregated black powder formed from reduction of  $MoCl_3(THF)_3$  was found to be  $Mo_2C$  by variable-temperature X-ray powder diffraction. Presently, we feel that it is unlikely that the carbide originates from the solvent (THF) since decomposition of the solvent is more likely to lead to metal oxide formation, and we currently suspect that  $LiBEt_3H$  may be the source of carbide. Consistent with this proposal, the reduction of  $MoCl_3(THF)_3$  with  $LiBH_4$  under the identical

(17) A representative example of the preparation of  $Mo_2C$  is presented here. Other reductions were carried out on a similar scale and no major differences were observed. Trichlorotris(tetrahydrofuran)molybdenum(III) (6.03 g, 14.43 mmol) was suspended in 150 mL of THF, which was cooled by ice/ $NaCl/H_2O$  cooling bath. Into this suspension, 50.0 mL of 1.0 M  $LiBEt_3H/THF$  was added slowly from a pressure-equalized dropping funnel. An immediate color change from red-brown to black accompanied by a gas evolution was observed. After 24 h of subsequent stirring at room temperature, the black suspension was centrifuged to give a black solid, which after washing with THF, EtOH, and THF was pumped to dry give 1.36 g of black powder  $Mo_2C$ , a yield of 93% based on  $MoCl_3(thf)_3$ . Elemental Anal. Calcd for  $Mo_2C$ : C, 5.88%; H, 0%. Found: C, 6.43%; H, 1.07%. From  $MoCl_4(THF)_2$ : Elemental Anal. Calcd for  $Mo_2C$ : C, 5.88%; H, 0%. Found: C, 6.32%; H, 1.04%.

reaction conditions to the  $\text{LiEt}_3\text{H}$  reduction reactions described above, did not result in formation of  $\text{Mo}_2\text{C}$  as determined by X-ray powder diffraction after heating the product to 500 °C.

We have observed that a key feature to the success of these experiments is the purity of the starting materials. When  $\text{MoCl}_3(\text{THF})_3$  is prepared according to the literature method<sup>18</sup> which involves reduction of  $\text{MoCl}_4(\text{THF})_2$  with tin powder, we have found that after reduction and separation, traces of tin were always incorporated in the final product as determined by energy-dispersive spectroscopy. As part of these studies, we have recently reported<sup>19</sup> a single-step method for the preparation of high-purity  $\text{MoCl}_3(\text{THF})_3$  in high yield by the reduction of  $\text{MoCl}_5$  with 2 equiv of diphenylsilane. Further studies are in progress to unambiguously determine the origin of the carbide in these materials and to explore the generality of this reduction method.

**Acknowledgment.** We thank the Office of Naval Research, Chemistry and Department of Materials Research for funding this research and the National Science Foundation Chemical Instrumentation program for the purchase of a low-field NMR spectrometer. We thank Dr. A. Datye for TEM data.

**Registry No.**  $\text{Mo}_2\text{C}$ , 12069-89-5;  $\text{W}_2\text{C}$ , 12070-13-2;  $\text{MoCl}_2(\text{THF})_3$ , 31355-55-2;  $\text{MoCl}_4(\text{THF})_4$ , 16998-75-7;  $\text{WCl}_4$ , 13470-13-8;  $\text{LiEt}_3\text{H}$ , 22560-16-3.

(18) Dilworth, J. R.; Zubieta, J. A. *Inorg. Synth.* 1986, 24, 192-194.

(19) Zeng, D.; Hampden-Smith, M. J. *Polyhedron*, in press.

## Novel Liquid-Crystalline Polymeric Materials via Noncovalent "Grafting"

C. Geraldine Bazuin\* and Frank A. Brandys

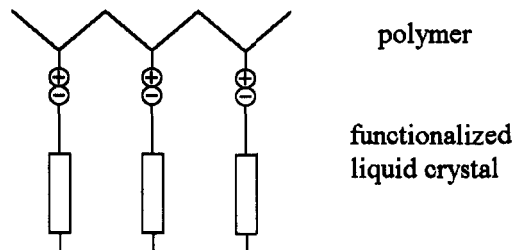
Centre de recherche en sciences et ingénierie des macromolécules (CERSIM), Département de chimie Université Laval, Québec, Canada G1K 7P4

Received May 7, 1992

Revised Manuscript Received July 9, 1992

Traditionally, liquid-crystal (LC) polymers have been classified as main-chain or side-chain types.<sup>1,2</sup> In an attempt to better account for the variety in these materials, which now include examples which cannot be classified as strictly side-chain or main-chain, Brostow<sup>3</sup> has proposed a classification scheme based on different architectural arrangements of the structural subunits forming the LC polymer. Twenty classes have been identified.

It is striking that in all cases the structural subunits are connected by covalent bonds. We would like to suggest that the variety in LC polymers can be considerably extended through the use of *noncovalent* bonds of various types. These noncovalent bonds can be formed by hydrogen bonding interactions, electrostatic interactions (e.g., ion-ion, ion-dipole, charge transfer), and coordination complexes or transition-metal ions. An idealized schematic of this concept, illustrated for ion-ion bonding and for a classical side-chain polymer architecture, may be shown as follows:<sup>4</sup>

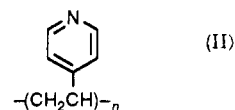
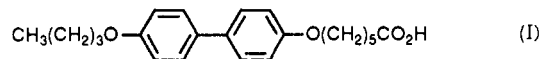


To achieve this end, a typical low molar mass liquid crystal must be functionalized with an ionic or ionizable functional group and mixed with a polymer possessing complementary ionic or ionizable groups.

An application of this concept has been published recently by Ujiie et al.<sup>5</sup> They have shown that the mixing of an ammonium cation-functionalized liquid crystal with sulfonate-type anionic polymers, which results in ion-ion interactions, indeed produces a material which exhibits thermotropic liquid-crystalline phases, and that the thermal stability of the phases are enhanced in the mixture. Furthermore, Fréchet and co-workers<sup>6,7</sup> have demonstrated that hydrogen bonding can be effective in forming or in extending mesogen cores, thus creating and stabilizing, respectively, liquid-crystalline phases. In the first case,<sup>6</sup> dimers of alkoxybenzoic acid side chains (attached covalently to the polymer backbone) are formed through hydrogen bonding, thus creating a mesogenic core of sufficient length to allow the formation of liquid-crystalline phases. The second case<sup>7</sup> involves hydrogen bonding between the same alkoxybenzoic acid side chain and a pyridine group which is located at one end of a small-molecule liquid-crystalline rigid core. The last example approaches the idealized schematic illustrated above but with the noncovalent interaction located within the rigid core rather than near the polymer backbone.

In this communication, we present our first results for a mixture of a simple low molar mass liquid crystal, functionalized at the end of the alkyl chain spacer by a carboxylic acid group, with poly(4-vinylpyridine) (P4VP). Hydrogen bonding interactions are expected between the acid and the vinylpyridine groups. These interactions are weaker than those exploited by Ujiie and co-workers; this has been illustrated, for instance, by the large difference in the effectiveness, in compatibilizing ionomer blends, of interactions between sulfonic acid and pyridine (where ion pairs are formed due to proton transfer) compared to those between methacrylic acid and pyridine.<sup>8</sup>

The functionalized liquid crystal (compound I), which we synthesized, and mixed with poly(4-vinylpyridine) (compound II), is based on a biphenyl core. This is di-



substituted by two *n*-alkoxy groups, one of which is terminated by the carboxylic acid group. To obtain the mixtures, the two compounds were dissolved and blended

(4) Preliminary results were presented at the Second Pacific Polymer Conference, Otsu, Japan, 1991 (preprints, p 205).

(5) Ujiie, S.; Iimura, K. *Macromolecules* 1992, 25, 3174; *Chem. Lett.* 1991, 411.

(6) Kumar, U.; Kato, T.; Fréchet, J. M. J. *ACS Polym. Mater. Sci. Eng.* 1991, 64, 231.

(7) Kato, T.; Fréchet, J. M. J. *Macromolecules* 1989, 22, 3819.

(8) Bazuin, C. G.; Eisenberg, A. *J. Polym. Sci., Polym. Phys.* 1986, 24, 1021.

(1) Shibaev, V.; Platé, N. *Adv. Polym. Sci.* 1984, 60/61, 173.

(2) McArdle, C. B., Ed. *Side Chain Liquid Crystal Polymers*; Chapman and Hall: New York, 1989.

(3) Brostow, W. *Polymer* 1990, 31, 979.